Document downloaded from:

http://hdl.handle.net/10251/122516

This paper must be cited as:

Luján, JM.; Climent, H.; Arnau Martínez, FJ.; Miguel-García, J. (2018). Analysis of low-pressure exhaust gases recirculation transport and control in transient operation of automotive diesel engines. Applied Thermal Engineering. 137:184-192. https://doi.org/10.1016/j.applthermaleng.2018.03.085

The final publication is available at

https://doi.org/10.1016/j.applthermaleng.2018.03.085

Copyright Elsevier

Additional Information

Analysis of low-pressure exhaust gases recirculation transport and control in transient operation of automotive diesel engines

José Manuel Luján, Héctor Climent*, Francisco José Arnau, Julián Miguel-García

CMT Motores Térmicos, Universitat Politècnica de València, Spain

*Corresponding author: hcliment@mot.upv.es. Telephone: (+34) 96 387 76 50. Postal address: CMT Motores Térmicos. Universitat Politècnica de València. Camino de Vera s/n. 46022. Valencia. Spain.

Abstract

The objective of the study is to determine the behavior of the low pressure exhaust gas recirculation (LP EGR) transport phenomena in the intake manifold during engine transient operation. The investigation also analyzes the influence of the propagation of the pressure waves in the intake manifold on the engine performance. In this sense, there is a clear trade-off: long intake lines improve the engine volumetric efficiency at low engine speeds but delay the EGR transport in the system.

The experiments were performed on a test bench with a 1.6 liter Euro-5 specification diesel engine. A CO_2 fast tracking measurement device was setup and placed in two locations in the intake line in order to track the EGR transport in transient operation. The CO_2 concentration is acquired with crank-angle resolution. Three different engine transients at constant engine speed were studied. They are extreme and worst-case scenarios in driving situations: (i) from low load to full load, (ii) from full load to low load, and (iii) from low load to medium load. In this way, it is possible to observe the behavior of the engine when: (i) leaving the EGR zone, (ii) entering into the EGR zone, and (iii) changing operating point without leaving the EGR zone.

A consistent methodology that combines experimental results and a 1D model capable to predict the behavior of the engine was developed. The results obtained in this investigation show a relevant phenomenon: depending on the synchronization of the EGR and Exhaust Throttle (ET) valves, an overshoot occurs when the engine enters into EGR zone. In this study, the results show the importance of the synchronization of the valves that control the EGR strategy. Comparisons between measured and modeled CO_2 concentrations lead to conclude that the EGR transport during engine transient operation is correctly predicted within a 1D engine code.

1. Introduction

The development of current diesel engines is focused on lowering fuel consumption and pollutant exhaust emissions. Since pollutant emission regulations have become more restrictive, new technologies are being developed. Exhaust gas recirculation (EGR) strategy is widely used in diesel engines due to the benefit in NOx emissions [1, 2]. As the limit of NOx emissions become more stringent, the EGR rates increase and strategies become more complex. The introduction of exhaust gases in the combustion

chamber inhibits the creation of NOx emissions by reducing the peak combustion temperature and decreasing the oxygen concentration.

The disadvantages of the EGR have been studied since decades, mainly the soot increase [3]. It has been studied the effects of the EGR temperature on diesel engines combustion and emissions [4]. The need to reduce NOx emissions has forced to increase the EGR rates, develop more complex strategies and create after-treatment systems.

Nowadays new after-treatment systems such as Selective Catalytic Reduction (SCR) based in Urea Water Solutions (UWS) have been developed. The UWS is injected in the exhaust to react with NOx and reduces signally the NOx. Nonetheless this system presents some disadvantages as the deposits of urea and its byproducts during cold weather conditions and low exhaust temperatures [5], and the economic spending to load the tank with UWS. Moreover after-treatment systems entails a penalty of fuel consumption because of the increase of the back-pressure.

In spite of the new after-treatment systems, the development of new and more complex EGR strategies are necessary. The simultaneous use of HP and LP EGR is a recent strategy to reduce NOx emissions and fuel consumption at low and medium speed and load conditions. However, LP EGR is especially useful at high loads and in transient operations [6]. EGR strategies in gasoline engines have been studied to reduce fuel consumption and NOx emissions. In addition, EGR in gasoline engines can replace fuel enrichment and avoid the knock [7]. Moreover the comparison between HP and LP cooled EGR in turbocharged gasoline engines have been studied. HP or LP EGR must be applied depending on the operation point of the engine [8]. Including the application of EGR in alternative (liquid and gaseous) fuels like raw oils, processed oils, hydrogen or natural gas have been studied too [9].

This study is focused in the LP EGR configuration. In one hand, LP EGR presents some disadvantages versus HP EGR. LP EGR transport takes more time to arrive to the cylinders due to the length of the intake line, produces higher hydrocarbon (HC) emissions and, at cold conditions, presents lower efficiency than HP EGR since it increases the intake temperature [10]. In addition, LP configuration needs more exhaust energy because the compressor operates under higher amount of gas. In the other hand, LP EGR shows some advantages compared to HP EGR [11]. HP EGR reduces NOx emissions but penalizing the fuel consumption and the dispersion of the EGR among cylinders, which can have consequences for NOx and PM emissions [12]. As to LP EGR loop systems are effective means of simultaneously reducing the NOx emission and fuel consumption [13]. Moreover, with LP EGR loop systems, the gas flow through the turbine is unchanged while varying the EGR rate [14]. However, if very high EGR rates are desired, it is sometimes necessary to close a backpressure valve placed in the exhaust line, which is usually referred to as exhaust throttle (ET) valve.

The tendency of the new homologation cycles, such as the Worldwide harmonized Light vehicles Test Cycles (WLTC) and Real Driving Emissions (RDE) cycles, will be more restrictive with transient operation which are more pollutant. For that reason, in parallel with the new homologation cycles, it is necessary to improve the control of emissions in transient operations [15].

Experimental and modeling tools were employed to fulfil this study. Traditionally, experimental tests have been combined with modeling results because there are some parameters in the engine that are impossible or complex to be measured [16]. The instantaneous gas concentration or instantaneous mass flow in a certain location during a given engine transient are good examples.

The paper is structured as follows: In Section 2 the experimental setup is explained. Section 3 is devoted to the explanation of modeling tools. Section 4 contains main results and discussion in terms of gases transport in the intake line for different transients and intake line configurations, synchronization of the EGR and ET valves, and the overshoot phenomenon. Finally, summary and main conclusions are presented in Section 5.

2. Experimental setup

The experiments were performed on a test bench with a turbocharged diesel engine, which is Euro-5 compliant. Table 1 shows the main features of the engine. The engine includes both LP and HP EGR systems. This study is focused in the LP EGR loop of the engine, whose schematic layout is depicted in Fig. 1. There are two intake line configurations depending on the length of the duct between the charge air cooler and the intake manifold. The first configuration is the original one, while the second includes an additional 600 mm length pipe. The aim is to analyze the influence of the intake line acoustics. The transients were performed with an ECU-controlled movement of the EGR valve. If the desired EGR rate is not achieved with the EGR valve fully open, it is necessary to regulate with the ET.

Table 1

Engine specifications.

Cylinder number	In-line 4
Bore x stroke (mm)	80x79.5
Displacement (cm^3)	1600
Compression ratio	15.4:1
Valve number	4/cylinder
Fuel delivery system	Common rail. Direct injection.
EGR system	HP EGR and LP cooled EGR
Intake boosting	Turbocharger with VGT
Intake cooling system	Air charge air cooler (ACAC)
Maximum power (kW/rpm)	96/4000
Maximum torque (Nm/rpm)	320/1750

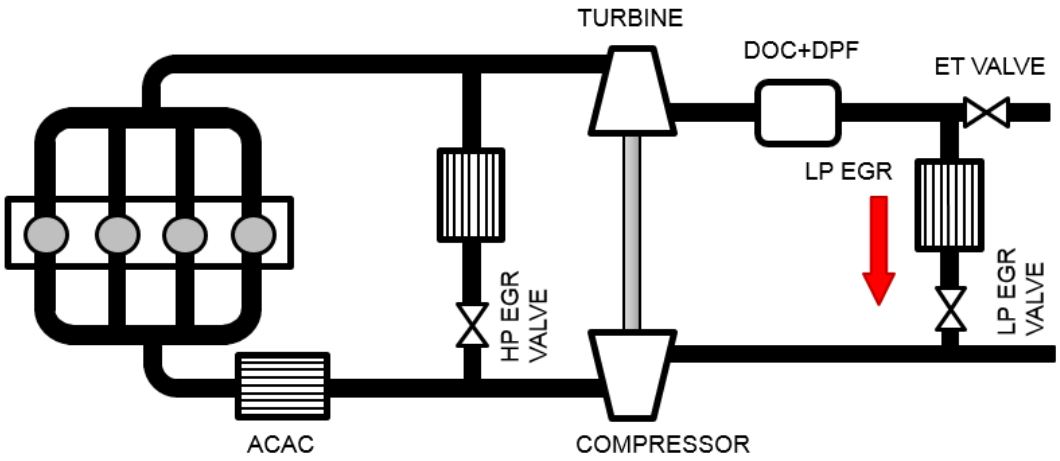

Figure 1. Engine schematic layout

A CO_2 fast tracking system, based on Non-Dispersive Infra-Red measuring principle, was used to evaluate the transport of exhaust gases in the intake line [17, 18]. The CO_2 tracking system is able to detect changes in gas concentration with a T_{90} of 8 ms, which is a higher sampling frequency than other conventional gas analysis systems, like the HORIBA MEXA 7170DEGR, often used in engine testing and widely used in steady operation. Moreover, the probe of the device can be placed in locations where quick changes in the gas pressure may occur, such as in the intake manifold during transient operation. The proposed experimental tests have been performed with high pressure gradients, i.e. from 1 to 2.6 bar (abs) during the load transient.

The fast tracking system is able to measure with two probes at the same time. One of them was installed upstream the compressor (downstream the LP EGR mixer with the intake air). Tests were carried out with the other probe placed in different locations: at charge air cooler outlet and in the intake manifold.

Three type of engine transient tests were assessed. The first one corresponds to the classic engine load response at constant engine speed. The engine transient starts at low load, in an operating condition where the LP EGR strategy is enabled. Suddenly, the pedal is pushed to its maximum position (full load), where the engine does not work inside the EGR zone.

The second transient is similar to the first one, but the engine load is increased without leaving the EGR zone. The third transient is just the opposite of the first one: the engine starts at full load (outside the EGR zone) and, suddenly, the pedal is released and let the engine run in low load conditions performing LP EGR.

All these engine transients were run at constant engine speed due to its remarkable impact on the volumetric efficiency, which is affected by the pressure waves propagation phenomenon inside the intake manifold. Therefore, in order to avoid interactions between the intake acoustics and the EGR transport delay it was decided to remove the engine speed effect by keeping it constant during the transient tests. In addition, to account for this influence on the torque evolutions, tests were performed separately at different engine speeds (1250, 1500, 1750 and 2000 rpm) and two different intake lines.

For the sake of repeatability, the instantaneous transients were performed with an ECU automatic control of EGR and ET valves. The ET valve acts as a backpressure valve. It is placed in the exhaust line, downstream of the LP EGR inlet. The objective of this valve is to increase the EGR rate if it is not enough with the EGR valve fully open. It usually happens at low load and low speed engine conditions. At full load conditions or during the transient performance, the EGR strategy is usually avoided, since it is desired to allow the maximum air mass flow to enter into the cylinders. Therefore, the EGR valve is fully closed and the ET valve is fully open in these conditions. In a fast engine transient, although the final situation is inside the EGR zone, it is very likely that the EGR strategy is switched off in the first stage of the transient and activated in the final part. This leads to a fast operation of both EGR and ET valves in a very short period of time. The synchronization of these valves will affect the EGR transport phenomena from the exhaust to the intake manifold.

Several engine parameters were measured to assess the engine performance and analyze the EGR transport in the intake manifold. The variables together with the sensors features are presented in Table 2.

Table 2

Instrumentation accuracy

Sensor	Variable	Accuracy [%]	Range
Thermocouples type K	Temperature	1	0 ºC – 1260 ºC
Pressure sensor	Pressure	0.3	0 – 6 bar
Gravimetric fuel balance	Fuel mass flow	0.2	0 – 150 kg/h
Hot wire meter	Air mass flow	1	0 – 720 kg/h
Dynamometer brake	Torque	0.1	0 – 480 Nm
NDIR500 CO&CO_2 analyzer	CO_2	2	0 – 20 %

The pollutant emissions were measured with specific equipment (Horiba MEXA 7170DEGR), which acquires the NO_X, THC, CO, CO_2, and O_2 concentrations in the location where the probe is placed. The EGR rate has been obtained experimentally from CO_2 measurement in exhaust and intake manifolds [19] using the following expression:

$$EGRrate = \frac{[CO_2]_{Intake} - [CO_2]_{Ambient}}{[CO_2]_{Exhaust} - [CO_2]_{Ambient}} \quad (1)$$

3. Modeling tools

The flow behavior inside intake and exhaust systems of internal combustion engines can be simulated with computer tools. The flow is considered essentially one-dimensional inside the systems that conform the engine. This situation will be true only if the length-to-diameter is high enough and the turbulent flow is totally developed. The governing

equations for one-dimensional unsteady compressible non-homentropic flow, i.e the mass, momentum and energy conservation equations, from a hyperbolic system of partial differential equations in the vector from of Eq. (2). The vectors are represented in strong conservative form in Eq. (3):

$$\frac{\partial \mathrm{W}}{\partial \mathrm{t}} + \frac{\partial \mathrm{F}}{\partial \mathrm{x}} + C1 + C2 = 0 \tag{2}$$

Where W is the solution vector, F represents the flux vector (mass, momentum and energy), and C1 and C2 include the source terms that take into account the effects of heat transfer, area changes and friction. These vectors are expressed as:

$$\begin{aligned} W\,(x,t) &= \begin{bmatrix} \rho \mathrm{F} \\ \rho \mathrm{uF} \\ F\,\left(\rho \frac{u^2}{2} + \frac{p}{\gamma - 1}\right) \end{bmatrix} \\ F\,(W) &= \begin{bmatrix} \rho \mathrm{uF} \\ (\rho u^2 + \mathrm{p})\,\mathrm{F} \\ uF\,\left(\rho \frac{u^2}{2} + \frac{\gamma p}{\gamma - 1}\right) \end{bmatrix} \\ C1(x,W) &= \begin{bmatrix} 0 \\ -p\,\frac{dF}{dx} \\ 0 \end{bmatrix} \\ C2(W) &= \begin{bmatrix} 0 \\ g\rho F \\ -q\rho F \end{bmatrix} \end{aligned} \tag{3}$$

The flow properties can be obtained at every node of the duct and time instant considering different numerical methods, time marching and spatial discretization techniques in the solution of the Eq. (2) and the state equation of the ideal gases [20-23]. Moreover, it is likely to estimate the inclusion of the chemical species transport equation to the governing equations system with the same level of precision of the applied numerical methods and without changes in the solution procedure. It is required n-1 equations of chemical species conservation in the governing equations system, where n is the number of the chemical species to be transported, to solve the transport of the chemical species along the 1D elements. The chemical species conservation equation in vector form is

$$\frac{\partial(\rho YF)}{\partial t} + \frac{\partial(\rho uYF)}{\partial x} = \rho F\dot{\mathrm{Y}}, \tag{4}$$

where Y is a vector including the mass fraction of n−1 different chemical species. The mass fraction of the chemical species n is given by the compatibility equation

$$Y_n = 1 - \sum_{j=1}^{n-1} Y_j, \tag{5}$$

The effect of the conversion rate and the convective transport have been considered in Eq. (4) due to chemical reactions. Because of the negligible influence of the term owing to diffusion among the chemical species compared to the velocity transport in ducts of internal combustion engines, it is no considered. Bearing in mind the chemical species

transport in 1D elements, the governing equations system in vector and strong conservative form is formulated as [24]:

$$W(x,t) = \begin{bmatrix} \rho F \\ \rho u F \\ F\left(\rho\frac{u^2}{2} + \frac{p}{\gamma-1}\right) \\ \rho F Y \end{bmatrix}$$

$$F(W) = \begin{bmatrix} \rho u F \\ (\rho u^2 + p)\,F \\ uF\left(\rho\frac{u^2}{2} + \frac{\gamma p}{\gamma-1}\right) \\ \rho u F Y \end{bmatrix} \quad (6)$$

$$C1(x,W) = \begin{bmatrix} 0 \\ -p\frac{dF}{dx} \\ 0 \\ 0 \end{bmatrix}$$

$$C2(W) = \begin{bmatrix} 0 \\ g\rho F \\ -q\rho F \\ \rho F \dot{Y} \end{bmatrix}$$

The adaptation of the numerical methods is needed, due to the complexity of the equations system with chemical species. In this work it is used the two-step Lax-Wendroff method case [25] because it offers fast and good results to this type of study which does not analyze the internal part of the engine like combustion chamber or elements close to the cylinders.

Additionally to 1D elements, 0D elements are employed too. 0D elements are used as much as possible because the resolution of their equations consume less resources and are faster to solve. The characteristic of the 0D elements is that they can accumulate mass so that the flow conditions are constant throughout its volume at each calculation step. Such as the case of the turbine, cylinders, after-treatment devices, etc. These kinds of elements are solved by means of a filling and emptying model [26] that includes the mass and energy conservation equations for open systems combined with the ideal gas state equation.

The chemical species transport across 0D elements involves the addition of n−1 mass conservation equations to calculate the mass fraction of n − 1 chemical species,

$$\Delta m_{in_{Y_j}} = \sum_i \dot{m}_i Y_{jCC_i} \Delta t \quad (7)$$

where $m_{in_{Y_j}}$ is the mass of the chemical species j inside the 0D element and Y_{jCC_i} is the mass fraction of the chemical species j entering to or exiting from the 0D element through the boundary condition i. Finally, the mass fraction of the chemical species j at time instant will be

$$Y_j = \frac{m_{in_{Y_j}} + \Delta m_{in_{Y_j}}}{m_{in} + \Delta m_{in}} \quad (8)$$

As in the case of the 1D elements, the mass fraction of the chemical species n is given by the compatibility Eq. (5). The species considered in the model of the present study are air, burned gas and fuel.

Finally, other submodels may be used to account for the EGR, VGT and ET valves movement [27] although, in this study, the time evolution of every valve position was considered as an input to the model. This is a suitable approach since one of the objectives of the study is to assess the 1D model capability to reproduce the EGR transport in the intake line and not to develop a complex model of the valves actuation system.

4. Results and discussion

Once experimental and modeling tools have been explained, it is possible to analyze and discuss the results. It is important to differentiate three cases:

Influence of the intake line length

Fig. 2 presents the EGR valve position on the left, the ET valve position on the middle and the CO_2 concentration measured in the intake manifold on the right. Fig. 2 shows a comparison during the tip-in engine operation at 1250 rpm between the original configuration and the additional 600 mm length pipe. Since the transient starts in an engine running condition where the EGR strategy is active, the EGR valve is completely open to achieve the desired EGR rate. Once the engine is running steadily in low load situation the pedal is pushed at 0.5 seconds and a quick engine load transient is requested. Hence, the EGR valve closes and the ET valve fully opens because the ECU detects the transient situation. It is observed the immediate effect in CO_2 levels. That response verifies the capacity of the fast tracking system at detecting rapid changes in gas concentration. Later, that response will be compared with model results.

From the EGR emptying point of view there is not much difference between the original duct and the configuration with an additional 600 mm pipe. A delay of nearly 20 ms is detected when the additional duct is used. The contribution of the additional duct to the overall intake line volume leads to an increase of 10% which explains the limited influence in the EGR emptying process.

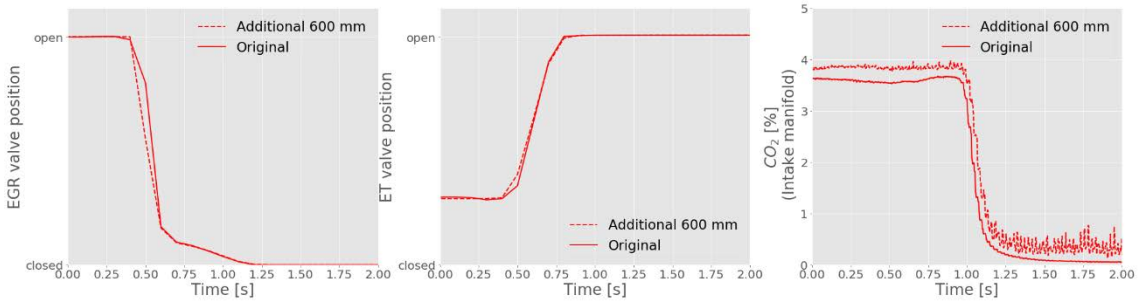

Figure 2. EGR (left) and ET (middle) valves movement and CO_2 evolution (right) in a tip-in transient operation at 1250 rpm with original intake line configuration and with the additional 600 mm duct.

Nevertheless, the intake manifold pressure shows differences during transient operation depending on the intake line length. Fig. 3 presents, on the left plot, higher intake pressure values when the additional 600 mm length duct is used (dashed line). Wave propagation phenomena is better tuned at 1250 rpm with the longest line. Engine tests without EGR have been performed to isolate both phenomena: EGR transport delay and pressure pulses propagation. It is observed in purple lines (without EGR) that the wave propagation presents a better transient response with the longest intake line (purple dashed line). Similar results are depicted in red (with EGR).

The smoke limiter strategy remained invariable during the testing campaign. However, since the objective of the study is to assess the influence of pressure wave propagation and EGR transport in the engine performance, the injected fuel gets modified if the air mass flow evolution changes from one configuration to another, and so the engine torque. Fig. 3 also shows the engine torque evolution on the right. The initial peak in the torque evolution does not have a relation with the engine behavior but with the control of the brake. Since a sudden change in the pedal position is requested and the transients have to be performed at constant speed, the system that controls the brake overreacts leading to a peak in the brake torque, which is released immediately after.

The analysis is focused in the torque evolution after 1 s. At first, it is possible to detect in red lines (with EGR) that the torque increases faster in case of the shortest intake line (solid line) than in case of longest intake line (dashed line). However, once the emptying of the EGR effect has finished, the longest intake line surpasses the shortest one due to the wave propagation phenomenon. In purple lines (without EGR) the effect in the early stage of the transient is similar with both intake line lengths. It happens because the EGR is not activated. However, it is observed how the wave propagation phenomenon appears as the transient evolves, promoting a better transient with the longest intake line.

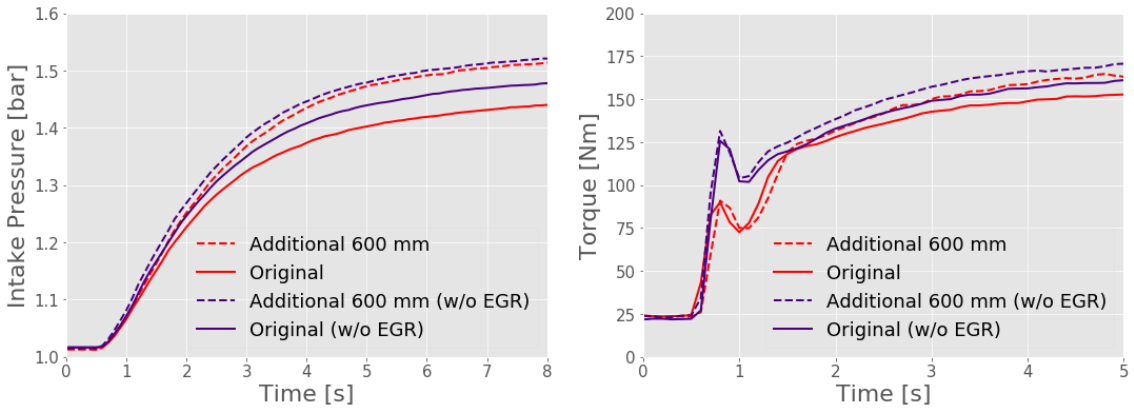

Figure 3. Intake pressure (left) and torque evolution (right) during a tip-in transient operation at 1250 rpm with original intake line configuration and with the additional 600 mm duct, with EGR strategy and without EGR strategy.

At a higher engine speed, 1750 rpm, Fig. 4 shows the intake manifold pressure during the engine load transient on the left. Concerning the tests without EGR (in purple), the original duct provides a faster response. The original line is better tuned in terms of pressure waves propagation at this engine speed than the longest line. Similar comments can be stated for the transients with EGR (in red), where a faster pressure rise is achieved with the shortest line. In the right plot of Fig. 4 the torque evolution is presented too. In this case, it is still observed that the beneficial effect of the wave propagation becomes relevant with the shortest line, as it has been demonstrated in the tests without EGR (purple lines). Engine torque evolution in tests with EGR is fastest with the shortest line too. In addition to the effect of the wave acoustics, there is also the quickest EGR emptying with the shortest intake line, which leads to a more rapid torque recovery in the early stages of the transient.

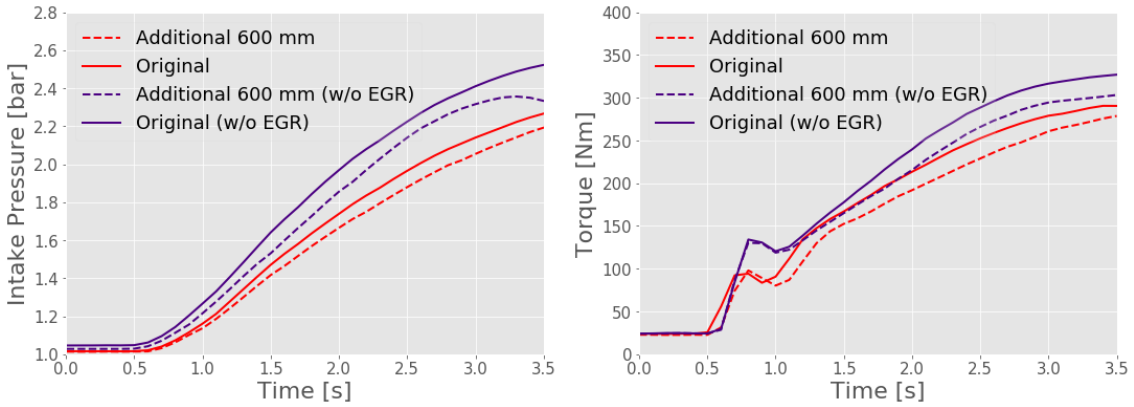

Figure 4. Intake pressure (left) and torque evolution (right) during a tip-in transient operation at 1750 rpm with original intake line configuration and with the additional 600 mm duct, with EGR strategy and without EGR strategy.

Fig. 5 presents a comparison between measurements and predicted results by the 1D engine model at 2000 rpm during the tip-in load transient. The plots correspond to the EGR valve position on the left, the CO_2 concentration at the compressor inlet in the middle and the CO_2 concentration in the intake manifold on the right. As commented previously, the valve position for the 1D model is directly imposed from the experimental data. The highly-scattered signal in the compressor inlet is due to the mixing of the exhaust gas coming from the exhaust line with the fresh intake air coming from the air filter. The mixture is far from being homogeneous despite the presence of an EGR mixing device and this explains its high variability captured by the gas analyzer. Results show a delay in the CO_2 concentration measurements between compressor inlet and intake manifold because of the length of the intake line. In this transient maneuver, the CO_2 takes about 0.4 seconds to disappear completely from the intake line since the EGR valve closes.

Secondly, it is observed that the calculated results are very close to the experimental results. These results show that the model can predict the reality and it is concluded that, for this type of EGR transport, the model is valid. The initial increase in the CO_2 concentration measured in the intake line is not realistic so an issue related to the device behavior due to the large intake pressure variations might be happening. Anyway, a good model response to the EGR transport phenomenon is found when leaving the EGR zone.

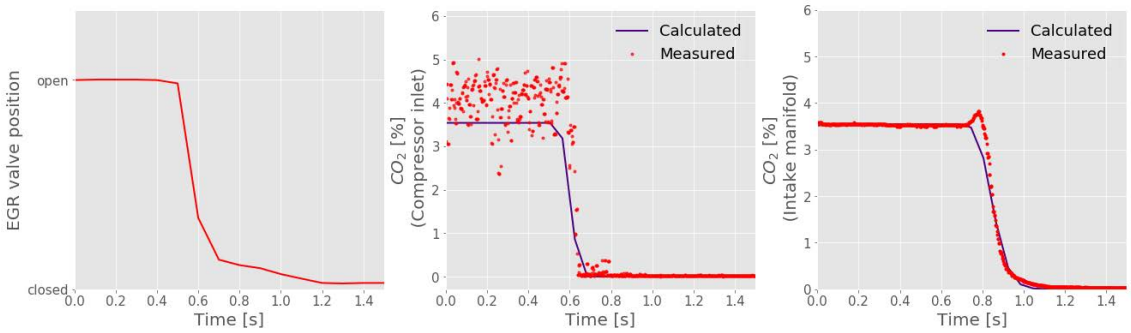

Figure 5. EGR valve movement (left) and comparison between measurement and predicted results by 1D model of the CO_2 evolution at the compressor inlet (middle) and in the intake manifold (right) in transient operation from 2 bar BMEP to full load at 2000 rpm.

Influence of the EGR and ET control

Fig. 6 presents, on the left, the valves position (the EGR on top and the ET at the bottom) and, on the right, the CO_2 concentration at the compressor inlet (top) and at the intake manifold (bottom). In this case it is observed the effect of entering in the EGR zone, from full load to 2 bar BMEP, at 2000 rpm. Regarding the measurement of the movement of the valves, in this tip-out operation the control strategy makes the EGR to open completely and enables the EGR strategy control to the ET valve. This valve, in a first phase, starts to close but an immediate opening peak is observed, followed again by a closing evolution up to the final position. If the ET valve would have moved directly to the final position, a remarkable CO_2 concentration overshoot would have occurred, as described in the following paragraphs. It is the opening movement of the ET valve in the middle of the transient, the responsible of reducing the overshoot effect shown at the beginning of the transient and depicted in the graphs on the right.

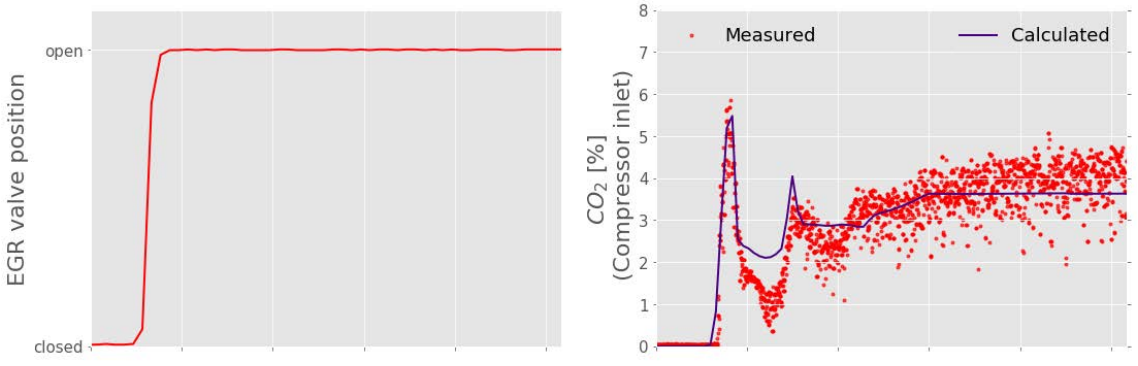

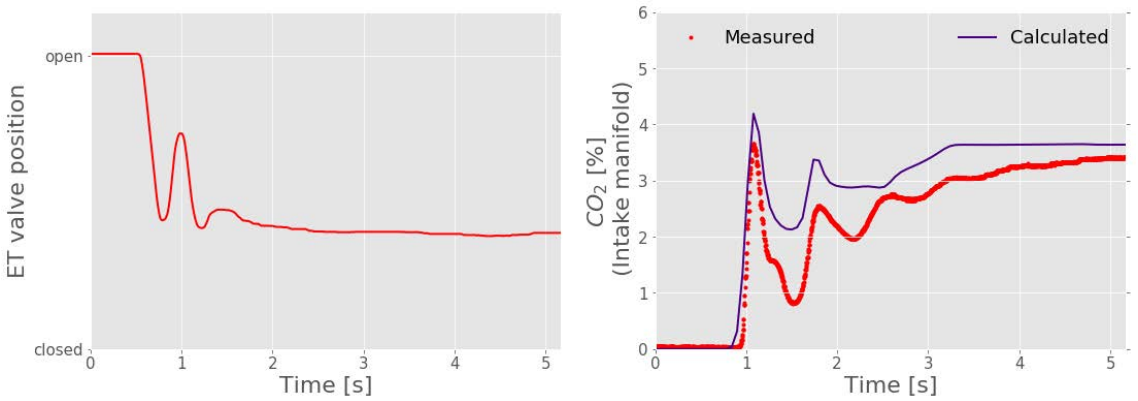

Figure 6. EGR (top left) and ET (bottom left) valves movement and comparison between measurement and predicted results by 1D model of the CO_2 evolution at the compressor inlet (top right) and in the intake manifold (bottom right) in transient operation from full load to 2 bar BMEP at 2000 rpm.

Fig. 7 shows, as previously, the valves position on the left, EGR on top and ET at the bottom. While on the right, it presents the CO_2 concentration at the compressor inlet on top and the CO_2 concentration in the intake manifold at the bottom. In this case the transient occurs inside the EGR zone, from 2 bar to 11 bar BMEP at 2000 rpm. As in the transient to full load, it is also observed that the ECU commands a closing of the EGR valve at the initial part of the transient in the top left plot and an opening of the ET valve at the bottom left plot. Later, since the engine remains inside the EGR zone, the EGR valve is again open and the ET performs the control of the air mass flow.

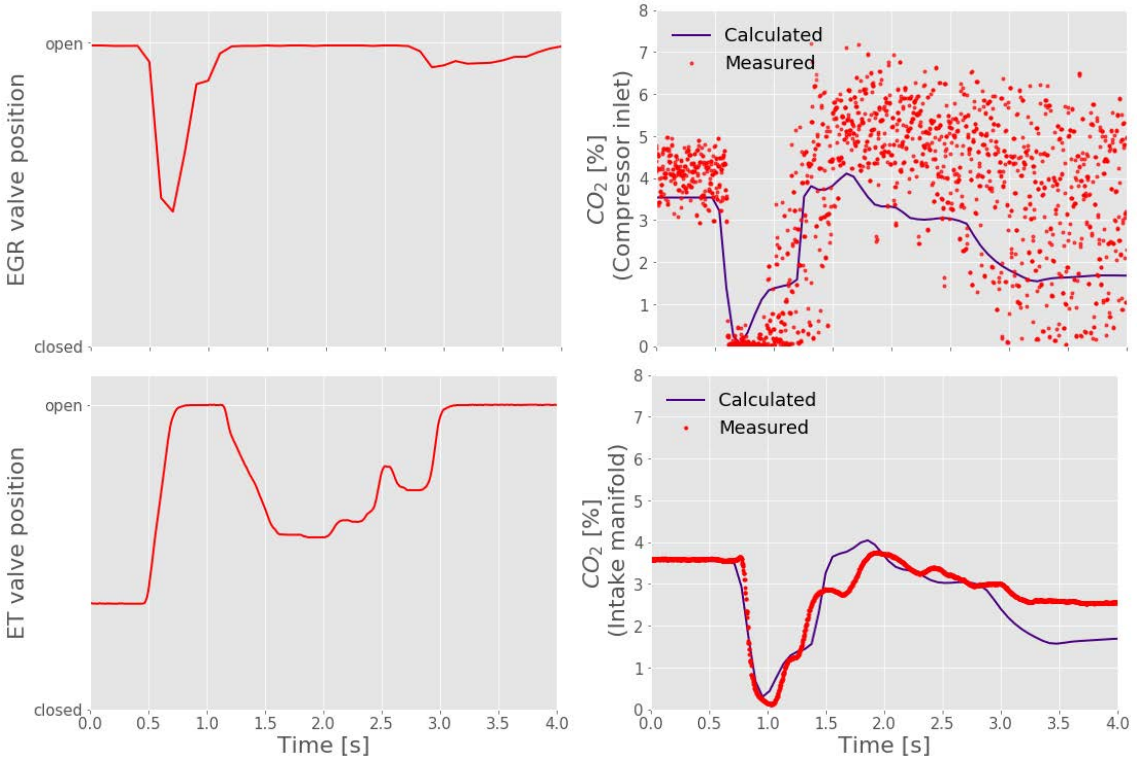

Figure 7. EGR (top left) and ET (bottom left) valves movement and comparison between measurement and predicted results by 1D model of the CO_2 evolution at the compressor

inlet (top right) and in the intake manifold (bottom right) in transient operation from 2 bar to 11 bar BMEP at 2000 rpm

The calculated results by the engine model are presented in Fig. 6. As in the experimental data, the overshoot phenomenon when entering in the EGR zone is properly captured. On the left plots of Fig. 6 and 7, the position of the EGR and ET valves in the model are the same as in the tests, since the movement of the valves in the model is imposed from the experiments. The model performance when predicting the CO_2 concentration along the intake line is observed in the plots on the right of Fig. 6 and 7. Both concentrations, at the compressor inlet and in the intake manifold, are very similar to measured data during the early stages of the transient (between the period of 0.5 s and 2.5 s), which is the relevant phase of the present study.

The left plot in Fig. 8 shows the pressure at the inlet and outlet of the LP EGR system in the transient from full load to 2 bar BMEP at 2000 rpm. Fig. 8 demonstrates that the overshoot is caused because in the first stage of the transient, in full load steady operation, the exhaust pressure is much higher than the inlet compressor pressure. In this situation the EGR valve is completely closed. The pressure at the inlet of the LP EGR system (exhaust line) is high due to the pressure loss in the exhaust line when the mass flow through the engine is very high. On the contrary, the pressure at the outlet of the LP EGR system (compressor inlet) is low due to the high pressure loss in the air filter as a result of the high air mass flow through the engine. In the final part of the transient, in low load conditions, both pressure traces are closely related since the EGR valve is fully open. In fact, the pressure difference is the pressure loss in the EGR line due to the EGR mass flow. During the transient, there is an initial phase where both pressures approach to each other very rapidly, indicating that the EGR mass flow has an important value.

The plot of the right shows the mass flow evolutions in three locations: at the outlet of the air filter (green), through the compressor (purple) and through the EGR valve (red). The large difference between exhaust and intake pressure together with the rapid opening of the EGR valve promotes a large amount of exhaust gases through the EGR line, which is the root cause of the EGR overshoot in the intake manifold. There is no need to close the ET at the same time as the EGR valve opens because of the initial EGR overshoot. In the last part of the transient, once the exhaust and intake pressures are closer, EGR mass flow goes down and it is necessary to close the ET to recover the EGR rate.

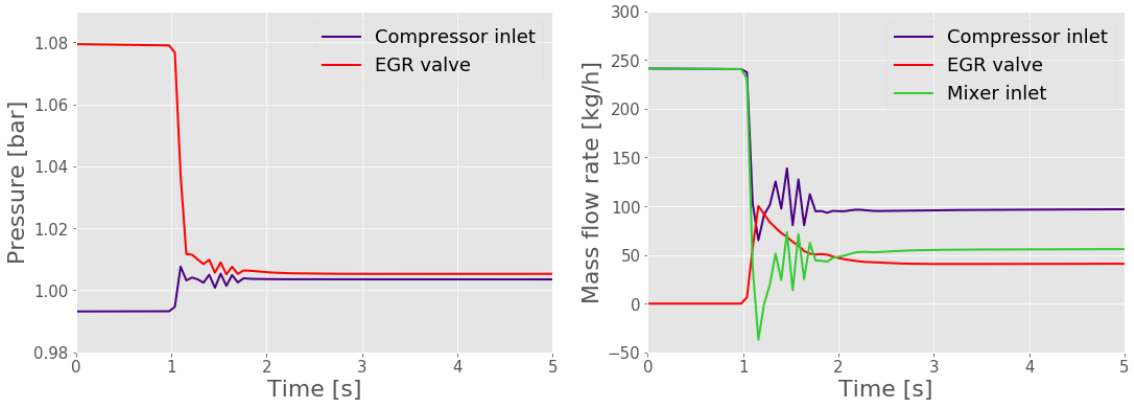

Figure 8. Pressure inlet and outlet of LP EGR system (left) and mass flow rate evolutions (right) in the transient from full load to 2 bar BMEP at 2000 rpm.

In order to check the impact of the synchronization between the EGR and the ET valves, a simulation, where the ET moves one second later than the opening of the EGR valve, is performed. Simulation results are shown in Fig. 9 comparing the original synchronization (in red) with one second delay (in purple). Fig. 9 presents on the left the movement of the valves (EGR valve on top and different synchronization of the ET valve at the bottom) and, on the right, the burned gas fraction (inlet of the compressor on top and in the intake manifold at the bottom). It is observed that when the ET closes at the same time as the EGR opens, an important EGR overshoot is created at the compressor inlet and is transported through the intake line up to the intake manifold and intake valves. In fact, there is no need to close the ET at the same time as the EGR valve opens because two effects are accumulated: (a) initial EGR increase due to the high value of exhaust-intake pressure difference and (b) the increase in the exhaust pressure due to ET valve partial closing. Fig. 9 shows that the delay in the opening of the ET valve reduces considerably the overshoot. The results of the combination of these two phenomena show that the synchronization of the EGR and ET valves is essential to reduce the overshoot phenomenon.

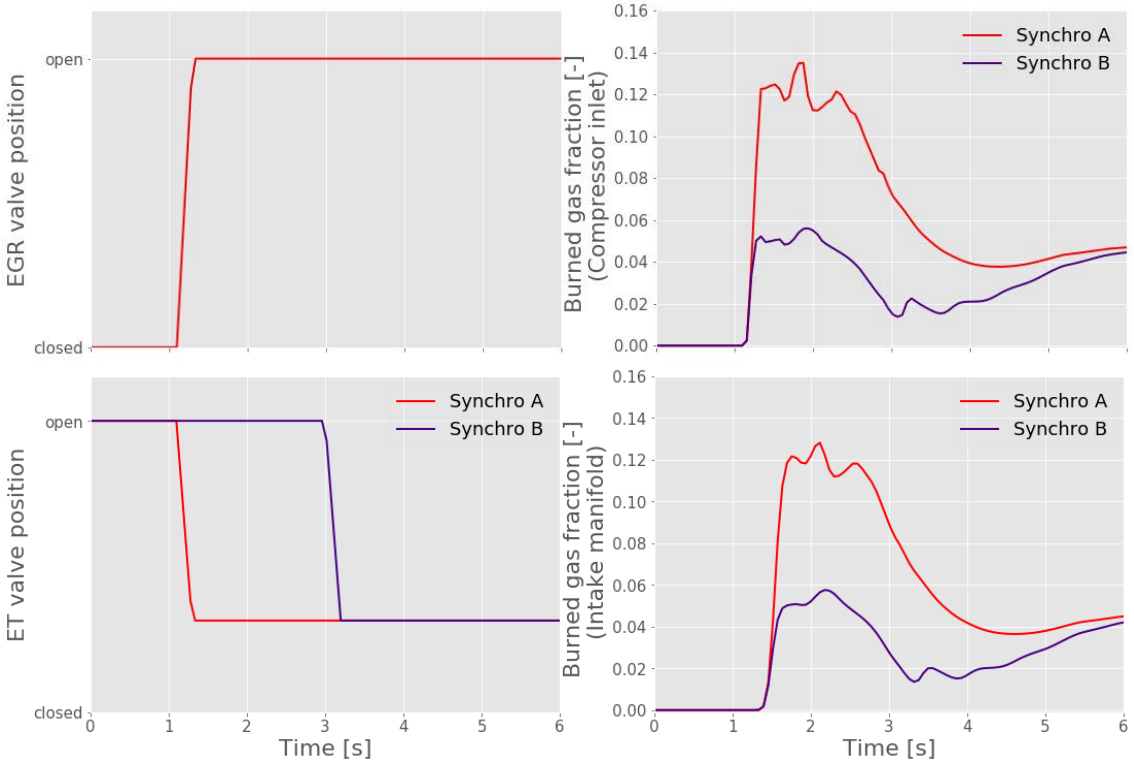

Figure 9. EGR (top left) and ET (bottom left) valves movement and comparison of the effect of different valve synchronization results given by 1D model of burned gas fraction at the compressor inlet (top right) and in the intake manifold (bottom right) in transient operation from full load to 2 bar BMEP at 2000 rpm

5. Summary and Conclusions

The tradeoff between wave propagation and the emptying of the EGR in engine load transients leaving the EGR zone was evaluated. Engine performance was assessed with two intake lines in transient operation at different engine speeds starting with and without EGR. Three different transients were tested at 1250, 1500, 1750 and 2000 rpm. It has been remarkable the role of the CO_2 fast tracking system, which has allowed to carry out the study because of its fast response and capability to measure under pressure variation conditions during transient operations.

At low engine speeds (i.e. 1250 rpm) the longest intake line was tuned and the wave propagation phenomenon is more effective in terms of engine torque than the effect of fast EGR emptying inside the intake line. When the engine speed increases, the longest intake line loses benefits due to both: not being acoustically tuned and higher volume to be emptied. Therefore, faster transients are achieved at higher engine speeds with the short intake line. Needless to say that the results may change with the specific application (mainly due to the dimensions and layout of the intake line), so special care should be paid when extrapolating the results. However, it is possible to say that, if the objective is to increase the performance of the engine in terms of torque evolution at low engine speeds, then, it is necessary to take into account wave phenomena probably with a longer intake line. In the other hand, if the objective is to increase the engine performance at high speeds, then, long intake line is not needed anymore and EGR transport is faster with a small sized intake manifold. In any case, the methodology is consistent and can be properly used in other situations.

An interesting result of this study has been able to quantify the delay of the exhaust gases transport in the intake manifold during the transient where the engine leaves the EGR zone, from 2 bar BMEP operation point to full load. The delay was quantified in 0.4 seconds at 2000 rpm since the EGR valve closing.

In case of entering into the EGR zone, it has been shown that the synchronization of the EGR and ET valves is very important to avoid or reduce the overshoot effect. It was demonstrated that a slower opening of the EGR valve or a delay in the closing of the ET valve helps to reduce significantly the overshoot.

A 1D model approach is valid for capturing the transport phenomena inside the intake line during transient operation in all performed cases because the evolution of the predicted CO_2 concentration is very similar to measured data. Moreover, it is very clear that the model is valid for any case as long as the position of the valves are correctly defined from the engine tests.

References

1. Ming Zheng, Graham T. Reader, J. Gary Hawley. “Diesel engine exhaust gas recirculation – a review on advanced and novel concepts.” Energy Conversion and Management 45 (2004) 883-900.

2. Deepak Agarwal, Shrawan Kumar Singh, Avinash Kumar Agarwal. “Effect of Exhaust Gas Recirculation (EGR) on performance, emissions, deposits, and durability of a constant speed compression ignition engine.” Applied Energy 88 (2011) 2900-2907.

3. Tokura, N., Terasaka, K., and Yasuhara, S., "Process through which Soot Intermixes into Lubricating Oil of a Diesel Engine with Exhaust Gas Recirculation," SAE Technical Paper 820082, 1982

4. Ladommatos, N., Abdelhalim, S.M., Zhao, H., “Effects of exhaust gas recirculation temperature on diesel engine combustion and emissions” Automobile Engineering 212 (1998) 479-500.

5. Sadashiva Prabhu S, Nagaraj S Nayak, N Kapilan, Vijaykumar Hindasageri. “An experimental and numerical study on effects of exhaust gas temperature and flow rate on deposit formation in Urea-Selective Catalytic Reduction (SCR) system of modern automobiles.” Applied Thermal Engineering 111 (2017) 1211-1231

6. Zamboni, G., Simone, M., Capobianco, M., “Hybrid EGR and turbocharging systems control of low NOx and fuel consumption in an automotive diesel engine.” Applied Energy 165 (2016) 839-848.

7. Wei, H., Zhu, T., Shu, G., Tan, L., Wang, Y., “Gasoline engine exhaust gas recirculation – A review.” Applied Energy 99 (2012) 534-544.

8. Shen, K., Li, F., Zhang, Z.,Sun, Y.,Yin, C., “Effects of LP and HP cooled EGR on performance and emissions in turbocharged GDI engine.” Applied Thermal Engineering 125 (2017) 746-755.

9. Thangaraja, J., Kannan, C., “Effect of exhaust gas recirculation on advanced diesel combustion and alternate fuels - A review.” Applied Energy 180 (2016) 169-184.

10. José Manuel Luján, Carlos Guardiola, Benjamín Pla, Alberto Reig. “Switching strategy between HP (high pressure) – and LPEGR (low pressure exhaust gas recirculation) systems for reduced fuel consumption and emissions.” Energy 90 (2015) 1790-1798.

11. Giorgio Zamboni, Massimo Capobianco. “Experimental Study of the effects of HP and LP EGR in an automotive turbocharged diesel engine.” Applied Energy 94 (2012) 117-128.

12. Alain Maiboom, Xavier Tauzia, Jean-François Hétet. “Influence of EGR unequal distribution from cylinder to cylinder on NOx-PM trade-off of a HSDI automotive Diesel engine.” Applied Thermal Engineering 29 (2009) 2043-2050.

13. José Manuel Luján, Héctor Climent, Benjamín Pla, Manuel Eduardo Rivas-Perea, Nicolás-Yoan François, José Borges-Alejo, Zoulikha Soukeur. “Exhaust gas recirculation dispersion analysis using in-cylinder pressure measurements in automotive diesel engines.” Applied Thermal Engineering 89 (2015) 459-468.

14. Alain Maiboom, Xavier Tauzia, Samiur Rahman Shah, Jean-François Hétet. “Experimental Study of an LP EGR System on an Automotive Diesel Engine, compared to HP EGR with respect to PM and NOx Emissions and Specific Fuel Consumption” SAE Int. J. Engines 2(2):597-610, 2010, doi:10.4271/2009-24-0138.

15. David Heuwetter, William Glewen, David Foster, Roger Krieger, and Michael Andrine. “Experimental Investigation of Transient Response and Turbocharger

519 Coupling for High and Low Pressure EGR Systems." SAE Int. J. Engines7(2): 977-
520 985, 2014, doi:10.4271/2014-01-1367

521 16. J. Galindo, J. R. Serrano, F. J. Arnau, and P. Piqueras. "Description of a Semi-
522 Independent Time Discretization Methodology for a One-Dimensional Gas
523 Dynamics Model." J. Eng. Gas Turbines Power 131(3), 034504 (Feb 10, 2009) (5
524 pages), doi:10.1115/1.2983015

525 17. Sutela, C., Collings, N., and Hands, T., "Fast Response CO2 Sensor for Automotive
526 Exhaust Gas Analysis," SAE Technical Paper 1999-01-3477, 1999,
527 doi:10.4271/1999-01-3477.

528 18. Sutela, C., Collings, N., and Hands, T. "Real Time CO2 Measurement to Determine
529 Transient Intake Gas Composition under EGR Conditions." SAE Technical Paper
530 2000-01-2953, 2000, doi:10.4271/2000-01-2953.

531 19. J. M. Luján, H. Climent, L. M. García-Cuevas, A. Moratal, "Volumetric efficiency
532 modelling of internal combustion engines based on a novel adaptative learning
533 algorithm of artificial neural networks" Applied Thermal Engineering 123 (2017) 625-
534 634.

535 20. J.R. Serrano, F.J. Arnau, P. Piqueras, A. Onorati, G. Montenegro. "1D gas dynamic
536 modelling of mass conservation in engine duct systems with thermal contact
537 discontinuities." Mathematical and Computer Modelling 49 (5–6) (2009) 1078–1088.

538 21. J. Galindo, J.R. Serrano, F.J. Arnau, P. Piqueras. "High-frequency response of a
539 calculation methodology for gas dynamics based on Independent Time
540 Discretization." Mathematical and Computer Modelling 50 (5–6) (2009) 812–822.

541 22. J. Galindo, J.R. Serrano, F.J. Arnau, P. Piqueras. "Description of a semi-
542 Independent Time Discretization methodology for a one-dimensional gas dynamics
543 model." Journal of Engineering for Gas Turbines and Power 131 (2009) 034504.

544 23. A.J. Torregrosa, J.R. Serrano, F.J. Arnau, P. Piqueras. "A fluid dynamic model for
545 unsteady compressible flow in wall-flow diesel particulate filters." Energy 36 (2011)
546 671–684.

547 24. J.R. Serrano, H.Climent, P.Piqueras, O.García-Alfonso, "Analysis of shock
548 capturing methods for chemical species transport in unsteady compressible flow."
549 Mathematical and Computer Modelling 57 (7-8) (2013) 1751-1759.

550 25. P.D. Lax, B. Wendroff. "Systems of conservation laws." Communications on Pure
551 and Applied Mathematics 17 (1964) 381–398.

552 26. J. Galindo, J.R. Serrano, F.J. Arnau, P. Piqueras. "Description and analysis of a one-
553 dimensional gas-dynamic model with Independent Time Discretization." in:
554 Proceedings of the Spring Technical Conference of the ASME Internal Combustion
555 Engine Division, 2008, pp. 187–197.

556 27. J Galindo, H Climent, C Guardiola and J Domenech, T. Modeling the vacuum circuit
557 of a pneumatic valve system. Journal of Dynamic Systems, Measurement, and
558 Control. Vol. 131(3), 2009.